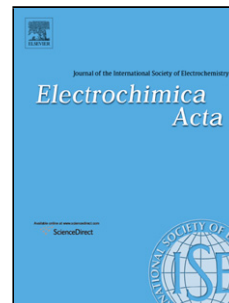


## Accepted Manuscript

Title: The chemical and electrochemical oxidative polymerization of 2-amino-4-tert-butylphenol

Author: M. Abidi S. López-Bernabeu F. Huerta F. Montilla S. Besbes-Hentati E. Morallón



PII: S0013-4686(16)31565-1  
DOI: <http://dx.doi.org/doi:10.1016/j.electacta.2016.07.060>  
Reference: EA 27675

To appear in: *Electrochimica Acta*

Received date: 20-2-2016  
Revised date: 26-4-2016  
Accepted date: 11-7-2016

Please cite this article as: M.Abidi, S.López-Bernabeu, F.Huerta, F.Montilla, S.Besbes-Hentati, E.Morallón, The chemical and electrochemical oxidative polymerization of 2-amino-4-tert-butylphenol, *Electrochimica Acta* <http://dx.doi.org/10.1016/j.electacta.2016.07.060>

This is a PDF file of an unedited manuscript that has been accepted for publication. As a service to our customers we are providing this early version of the manuscript. The manuscript will undergo copyediting, typesetting, and review of the resulting proof before it is published in its final form. Please note that during the production process errors may be discovered which could affect the content, and all legal disclaimers that apply to the journal pertain.

## The chemical and electrochemical oxidative polymerization of 2-amino-4-*tert*-butylphenol

M. Abidi<sup>1,2</sup>, S. López-Bernabeu<sup>2</sup>, F. Huerta<sup>3</sup>, F. Montilla<sup>2</sup>, S. Besbes-Hentati<sup>1</sup>, E. Morallón<sup>2</sup>

<sup>1</sup>*Laboratoire de Chimie des Matériaux, Faculté des Sciences de Bizerte. 7021, Zarzouna Université de Carthage, Tunisie.*

<sup>2</sup>*Dept. Química Física e Instituto Universitario de Materiales, Universidad de Alicante, Ap. 99, E-03080, Alicante, Spain*

<sup>3</sup>*Dept. Ingeniería Textil y Papelera, Universitat Politècnica de Valencia, Plaza Ferrandiz y Carbonell, 1. E-03801, Alcoy, Spain*

### Abstract

Poly(2-amino-4-*tert*-butylphenol), poly(2A-4TBP), was synthesized from monomer aqueous solution using either electrochemical or chemical oxidation procedures. Several spectroscopic characterization techniques were employed to gain information on the chemical structure and redox behavior of the obtained materials. It was found that the chemical polymerization product could be described as an oligomer mixture containing up to 16 monomer units. In parallel to other polymers derived from *o*-aminophenol, phenoxazine rings constitute also the basic structure of poly(2A-4TBP). In addition, the occurrence of N-N couplings, which are favored by the presence of the voluminous *tert*-butyl substituent, seems also relevant. No significant structural differences were found between the chemically or electrochemically synthesized materials.

Keywords: electrochemical polymerization; in situ FTIR; polyaminophenol

## 1. Introduction

Aminophenols constitute an interesting class of compounds for electropolymerization owing to the presence of reactive amino and hydroxyl units. It has been reported that the relative position of these units at the aromatic ring plays a significant role in the electrochemical reactivity of the molecule and, consequently, the electrochemical behavior of the three positional aminophenol isomers, *ortho*-, *meta*- and *para*-, is quite different [1–3]. Despite some early controversy on the formation, or not, of polymeric films from the electrochemical oxidation of *p*-aminophenol, it seems now proved that in aqueous media the monomer can be electropolymerized to yield complex oligomeric products whose chemical structure is strongly dependent on the pH of the working solution [4]. The electro-oxidation of *m*-aminophenol has been scarcely investigated because it yields an electroinactive polymer that blocks the electrode surface and shows a crosslinked structure similar to polyphenol [3,5]. On the contrary, it is well documented that *o*-aminophenol can be electrochemically polymerized in acidic medium to yield an electroactive polymeric material that shows phenoxazine ladder structures [3,6]. It was also suggested that the products formed upon *o*-aminophenol electrochemical oxidation depend on the pH of the polymerization solution [7] although it is worth noting that similar structure and properties can be obtained regardless of the polymerization method employed, either chemical or electrochemical [1].

Comparisons have been also made in the literature between chemical and electrochemical polymerization products obtained from other aromatic anilines, with special attention paid to diamines [8]. It is usually found that the chemical polymerization methods result in higher polymer yields although oligomeric by-products are difficult to remove from the reaction mixture. On the other hand, electrochemical polymerization offers the advantage that the fine control of the anodic potential avoids polymer overoxidation and, consequently, materials with less defects can be isolated on the electrode surface. The formation of non-conducting films upon electrochemical oxidation could prevent polymer growth and such a possibility should be taken into account mostly, although not exclusively, in experiments conducted in neutral and alkaline media.

Chemical and electrochemical polymerization of alkyl ring-substituted anilines has attracted interest because of the possibility to improve the poor solubility of unmodified polyaniline and, besides, to investigate the effect of blocking specific ring polymerization

sites with electron-donor substituents [9–11]. However, to the best of our knowledge, there is still no report dealing with the chemical or electrochemical polymerization of alkyl ring-substituted aminophenols. In the present work, an attempt has been made to synthesize a polymer from both routes and to analyze the effect of the presence of a voluminous alkyl group on the well-studied polymerization process of aminophenols. It is known that the presence of bulky groups attached to the aromatic ring may avoid  $\pi\pi$ -stacking between vicinal chains of the resulting polymer and this could lead to an improvement in solubility and processability of the resulting material. To achieve these goals, 2-amino-4-tert-butylphenol (2A-4TBP) has been selected as the monomer species and different spectroscopic techniques have been applied to the characterization of the oxidative polymerization products.

## 2. Experimental

The solutions employed for polymerization were 1.0 M HClO<sub>4</sub>, prepared from Merck Suprapur concentrated acid and 18.2 M $\Omega$  cm water obtained from an Elga Labwater Purelab system. 2-amino-4-tert-butylphenol monomer was purchased from Merck. Ammonium persulfate, from Merck, was used as the oxidant for chemical polymerization.

Cyclic voltammetry experiments were carried out in a conventional three-electrode cell under N<sub>2</sub> atmosphere. The working electrodes used were either platinum or ITO and a platinum wire was used as the counter electrode in all cases. All potentials were measured against the reversible hydrogen electrode (RHE) immersed in the working solution through a Luggin capillary. Cyclic voltammograms were recorded at a constant sweep rate of 50 mV s<sup>-1</sup> and at room temperature. The polycrystalline platinum electrodes were thermally cleaned and subsequently protected from the laboratory atmosphere by a droplet of ultrapure water. ITO electrodes were cleaned with acetone and ultrapure water. Chemically produced polymers were deposited on the working electrodes by casting a small volume of suspension containing 1 mg mL<sup>-1</sup> material in THF solvent.

*In situ* UV–Vis spectra of polymers were recorded with a V-670 spectrometer from JASCO, which is equipped with a double monochromator system and a photomultiplier tube detector. A Nicolet 5700 spectrometer equipped with a nitrogen-cooled MCT detector was employed for the *in situ* FTIR experiments. The working Pt disc electrode was mounted on a

glass tube and its 1.0 cm<sup>2</sup> surface was mirror-polished using alumina powder. The spectroelectrochemical cell was made of glass and was provided with a prismatic CaF<sub>2</sub> window beveled at 60°. Spectra were collected at 8 cm<sup>-1</sup> resolution in D<sub>2</sub>O solvent (from Aldrich with 99.9% D-atom purity) and are presented as  $\Delta R/R$ . XPS spectra were recorded with a VG-Microtech Multilab 3000 electron spectrometer using a non-monochromatized Mg-K $\alpha$  (1253.6 eV) radiation source of 300 W and a hemispheric electron analyzer equipped with nine channeltron electron multipliers. The pressure of the analysis chamber during the scans was about  $5 \times 10^{-7}$  N m<sup>-2</sup>. After the survey spectra were obtained, higher resolution scans were performed at pass energy of 50 eV. The intensities of the different contributions were obtained by means of the calculation of the integral one of each peak, after having eliminated the baseline with S form and adjusting the experimental curves to a combination of Lorentz (30%) and Gaussian (70%) lines. All the binding energies were referred to the line of the C 1s to 284.4 eV, obtaining values with a precision of  $\pm 0.2$  eV. The high-resolution mass experiments were performed in a MICROMASS Autospec spectrometer.

### 3. Results and discussion

#### 3.1. Electrochemically polymerized 2A-4TBP

Fig. 1 illustrates the cyclic voltammetry curves recorded for a polycrystalline platinum electrode immersed in 0.1 M HClO<sub>4</sub> + 15 mM 2A-4TBP solution. The oxidation of the monomeric species starts at 0.76 V and, as deduced from the high slope of the voltammetric curve, is kinetically favored during the first voltammetric sweep. The oxidation peak is centered at 0.87 V and, through the first reverse scan, two cathodic peaks are recorded at 0.8 V and 0.7 V. The former is clearly associated with the reversible reduction of oxidized species generated during the forward sweep, whereas the 0.7 V broad wave seems related with the

reduction of the oligomer products formed at higher potentials. Such products cannot be re-oxidized during successive forward sweeps, as manifested by the absence of anodic waves different from that of monomer oxidation. The peak current of the main oxidation feature decreases upon cycling and its initially fast kinetics decays gradually. Therefore, it is clearly deduced from the voltammetric profile that the anodic oxidation of aminophenol monomer yields electrochemically inactive oligomeric products that block the electrode hindering further oxidation. Cyclic voltammogram in Fig. 1b reveals that the blocking species are strongly adsorbed on platinum. This curve was recorded in a background electrolyte solution after 300 polymerization cycles, when the surface appeared covered with a purple film. The electrode was removed from the polymerization solution, washed with ultrapure water and transferred to the 0.1M HClO<sub>4</sub> test solution with no monomer added. The voltammetric curve shows the characteristic profile of a platinum electrode covered with a thin, almost electroinactive oligomeric film.

The featureless oxidation process undergone by poly(2A-4TBP) in Fig. 1b was monitored by *in situ* UV-vis spectroscopy in order to discern whether or not polaronic species are formed upon anodic polarization of this material. The polymer was deposited on an ITO coated glass electrode in a parallel experiment to that shown in Fig. 1a and then transferred to the spectroelectrochemical cell, where it was immersed at 0.05 V. *In situ* UV-Vis spectra were then recorded at increasing potentials and those obtained in the range from 0.05 to 0.65 V have been depicted in Fig.2.

The first UV-Vis spectrum collected at 0.05 V shows one main absorption feature at 558 nm. The intensity of this peak remains almost constant at potentials below 0.45 V but rises sharply above that value. Such a behavior suggests a redox transformation of the oligomeric material, with the absorption probably associated with a benzenoid-to-quinoid transition related to polaronic moieties formed upon electrochemical doping [12]. Such a band is slightly blue-shifted with respect to polyaniline and closer to the polaronic transitions observed for other ring-substituted polyanilines, indicating the presence of polaronic domains with short conjugated segments. However, the formation of quinone-like moieties upon oligomer oxidation could also contribute significantly to this band [13]. The occurrence of a

redox polaronic transformation in poly(2A-4TPB) is also supported by other spectral features in Fig 2. Specifically, the spectrum acquired at 0.65V shows the appearance of three additional bands centered at 397, 416 and 447 nm. The former one can be assigned to a polaron- $\pi^*$  transition, where polarons are isolated one from another reflecting low electrical conductivity of the oligomeric material [14]. Regarding the other two features it is worth mentioning that, according to literature data on polyaminophenols, electronic absorptions in the 410-450 nm range can be attributed to the progressive formation of radical cations in phenoxazine rings or, alternatively, to the occurrence of N-N coupling to form azobenzene derivatives [15–18]. In the present case, both structures are probably promoted by the presence of the voluminous tertbutyl group in *meta* position relative to the nitrogen atom, which tends to hinder the C-N *para*-coupling and hydrazine-type dimers could be formed due to such steric hindrance [19]. Finally, the band at 742 nm, whose intensity remains almost constant at increasing potentials, is of uncertain nature but it has been assigned either to the bipolaronic transition in *para*-coupled polyaniline derivatives or to the polaron transition in poly(*o*-aminophenols) [15,16]. According to these results, poly(2A-4TBP) seems an oligomeric product originated from a variety of C-N, C-O and N-N monomer couplings.

*In situ* FTIR spectroscopy has been used to confirm the existence of a redox transition in the electrochemically deposited poly(2A-4TBP). The filmed Pt electrode was transferred to the IR spectroelectrochemical cell, which contained a free of monomer test solution prepared with D<sub>2</sub>O to facilitate assignments in the 1500-1700 cm<sup>-1</sup> spectral range. After some potential cycles, the Pt surface was carefully pressed against the prismatic CaF<sub>2</sub> window, a reference spectrum was then collected at 0.1 V and, finally, the potential was stepped to higher values to collect sample spectra. By referring each sample to the unique reference, we can obtain information on the redox transformations undergone by the oligomeric material as a function of the applied potential. The computed *in situ* FTIR spectra are displayed in Fig. 3 within the frequency range 1100-2200 cm<sup>-1</sup>. There, the presence of several negative (downward) and positive (upward) bands reveals the activation of vibrational modes at increasing potentials, which is a characteristic behavior of reversible oxidation processes.

In fact, since no spectral features appear in the spectra obtained at 0.3 V and 0.4 V, it can be inferred that poly(2A-4TBP) cannot be oxidized at so moderate potentials. This observation is consistent with the results obtained from the *in situ* UV-vis experiments in Fig. 2. On the contrary, several IR absorption bands appear in the spectra collected from 0.5 V.

The onset of oligomer oxidation at around this potential is testified by the occurrence of a clear negative band at  $1613\text{ cm}^{-1}$ , a group of less intense negative absorptions in the  $1330\text{--}1400\text{ cm}^{-1}$  frequency range and, finally, two positive bands peaking at  $1518$  and  $1445\text{ cm}^{-1}$ . It can be observed that the integrated intensity of all these features, and therefore the oligomer oxidation level, increases at increasing potentials and, besides, new absorptions showing either negative or positive character are developing. Assignments proposed for the main bands are summarized in Table 1. Between the two main bands clearly related with the reduced form of poly(2A-4TBP), the feature appearing at  $1518\text{ cm}^{-1}$  can be unambiguously assigned to the progressive vanishing of the aromatic C-C stretching due to oligomer oxidation, whereas the peak at  $1312\text{ cm}^{-1}$  is related with the parallel transformation of secondary aromatic amines. The high intensity reached by the former feature is probably due to the presence of the electron-donor alkyl group in the aromatic ring [20]. The band at  $1445\text{ cm}^{-1}$  has been sometimes attributed to the skeletal C-C stretching vibration of the aromatic ring, although the interpretation of this band is not unanimous. Apart from the C-C stretching, it has been also ascribed either to the existence of N-N coupling or to the formation of phenazine structures in polyaniline derivatives [21,22]. In our case, owing to the presence of adjacent alcohol and amino groups, it is very likely the formation of phenoxazine rings and/or N-N coupling. This hypothesis seems supported by the *in situ* UV-vis results presented in Fig. 2.

With regard to the oxidized state, it is worth noting that the absorption bands appearing, roughly, below  $1600\text{ cm}^{-1}$  support the existence of a reversible redox transformation of poly(2A-4TBP). On the contrary, most features appearing above that frequency strongly suggest an irreversible degradation process of the oligomeric material at high potentials. Indeed, the reversible formation of quinoid rings and intermediate-order  $C\approx N$  bonds, which is common to most polyaniline derivatives, is confirmed respectively by the  $1578\text{ cm}^{-1}$  feature and the group of overlapped bands in the surroundings of  $1350\text{ cm}^{-1}$ . Quinone imine centers are responsible for the feature at  $1617\text{ cm}^{-1}$ , while the couple of negative-going bands at  $1750\text{ cm}^{-1}$  and  $1292\text{ cm}^{-1}$  supports the formation of carboxylic acid terminations and confirms the occurrence of an overoxidation process at potentials beyond  $0.9\text{V}$ . Furthermore, the negative band peaking at  $1650\text{ cm}^{-1}$  reveals the formation of degraded quinone structures at  $0.9\text{V}$  [3].



Electrodeposited poly(2A-4TBP) has been examined by *ex situ* XPS in order to give support to the chemical structures suggested by the *in situ* techniques. A film grown after 100 voltammetric cycles was rinsed with ultrapure water, dried under nitrogen and then analyzed by XPS. Fig. 4 shows the photoelectronic spectra of C 1s, N 1s and O 1s core levels. The C 1s signal can be fitted with a major peak at 284.6 and two minor peaks at 285.9 and 287.8 eV. The main role corresponds unambiguously to aromatic carbon, while the 285.9 eV contribution can be assigned to aromatic carbon bound to either amine or imine neutral nitrogen and also to oxygen-containing ether structures in the form of phenoxazine [25,26], which are not discernible. The binding energy of the negligible peak at 287.8 eV is probably too high to correspond to a carbonyl environment [27] and, consequently, it can be assigned better to a  $\pi$ - $\pi^*$  shake-up transition from the C 1s parent peak involving benzenoid rings. These signals are characteristic of low-conducting polymer systems showing extended unconjugated aromatic domains. With regard to the N 1s spectrum, it can be fitted with only two contributions showing maxima at 399.7 and 401.9 eV, respectively. The first one is attributed to neutral species that may correspond to amine, azo and imine groups, as these species do not show significantly different chemical shifts. The higher binding energy peak can be assigned to positively charged  $N^+$  atoms resulting from the protonation of imine centers [28,29], although the  $N^+/N$  ratio derived from Fig.4 is only 13%.

Finally, the O 1s core level spectrum has been deconvoluted into three peaks at 529.8, 532.3 and 533.6 eV. The intermediate feature at 532.3 eV can be assigned to quinone/carbonyl compounds [30], while the high energy peak at 533.6 eV is clearly related with the presence of C-O-C in phenoxazine species [26]. It is known that the O 1s main signal tends to be affected by spurious signals coming from extrinsic oxygen-containing species. Such an effect is particularly significant when samples are constituted by organic thin films deposited on Pt electrodes. This is the case of the 529.8 eV peak, which comes mostly from Pt-OH although a small contribution from carboxylic C=O species at over-oxidized polymer chains cannot be fully rejected. In essence, the XPS results presented in this section are compatible with the presence of both phenoxazine and azo-derivatives and support the assignments made above from *in situ* UV-vis and FTIR experiments.

### 3.2. Chemically polymerized 2A-4TBP

To carry out the chemical polymerization of 2-amino-4-tert-butylphenol, the compound was dissolved in 1.0 M HClO<sub>4</sub> until a concentration of 15 mM was attained. The polymerization was started after the addition of an equimolar ratio of ammonium persulfate in a vigorously stirred ice bath at 0°C. After 22 hours, the purple polymerization product was thoroughly washed with 1.0 M perchloric acid and then dried under dynamic vacuum for 3 hours. The material recovered after polymerization approaches 68%. For the electrochemical measurements, a platinum electrode coated with poly(2A-4TBP) was prepared by casting a drop of solution containing 1 mg/mL polymer on the metal substrate and then evaporating the solvent. Fig. 5 shows the stabilized cyclic voltammogram recorded in 0.1 M HClO<sub>4</sub> for such a modified electrode. The forward scan shows a broad anodic current centered at around 0.47 V while in the reverse scan the main reduction peak is centered at 0.42 V. No significant decrease in current has been recorded upon potential cycling, which indicates an adequate stability of the polymer film on this surface.

The oxidation process of poly(2A-4TBP) has been followed by *in situ* UV-vis spectroelectrochemistry. After chemical polymerization, the material was deposited on an ITO electrode and immersed in the perchloric acid test solution at controlled potential. Fig.6 shows the set of UV-vis absorption spectra recorded during a potential excursion from 0.05 V up to 0.65 V. Three absorption bands are detected at 385, 445 and 562 nm in the first spectrum of the series. The frequencies, and therefore the assignments, of these features fit well with those recorded in Fig. 2 for the electrochemically synthesized material. However, the intensity of the 562 nm feature in Fig. 2 rises faster at higher potentials, which is probably a consequence of the formation of additional species, specifically quinone-like groups, in the electrochemically deposited polymer. This observation strongly suggests that the electrochemically obtained material is more sensitive (i.e. is less stable) to the applied potential than the chemical one.

The chemically synthesized polymer conductivity has been measured by means of the four-probe method. The result was  $3 \times 10^{-8} \text{ S cm}^{-1}$ , a figure roughly between 10 and 30 times smaller than for poly(*o*-aminophenol) and about three orders of magnitude less than the alkyl Pani-derivative poly(*o*-toluidine). Interestingly, the *in situ* UV-vis spectra of poly(*o*-aminophenol) [15] shows a transient species formed at around the formal potential that seems at the origin of the polymer conductivity. The *in situ* UV-vis experiments shown in Figs. 2 and 6 reveal that the transient species is not formed or, maybe, its concentration is too low to

be detected. Consequently, the conductivity of poly(2A-4TBP) is significantly lesser than that of poly(*o*-aminophenol).

Possible structural and/or chemical singularities of poly(2A-4TBP) formed through the chemical route were examined by *in situ* FTIR spectroscopy. The platinum disc electrode was prepared, as in the previous experiment, by casting a drop of the dissolved polymer on its surface. The modified electrode was transferred to the spectroelectrochemical cell, where a reference spectrum was acquired at 0.1 V. The potential was then stepped sequentially to higher values to acquire sample interferograms. Fig.7 displays the *in situ* FTIR spectra recorded in 0.1M HClO<sub>4</sub>/D<sub>2</sub>O medium. Several absorption peaks, whose intensities increase at increasing potentials, were observed during potential scanning, showing the progress of the oxidation process.

In contrast to Fig. 3, FTIR spectra in Fig. 7 look dominated by negative-going features. The presence of several absorption bands peaking at 1507 cm<sup>-1</sup>, 1280 cm<sup>-1</sup> and 1190 cm<sup>-1</sup> in the first spectrum reveals that poly(2A-4TBP) electrochemical oxidation starts at potential values as low as 0.3 V. In addition, both the negative character and increasing intensity at higher potentials show these vibrational modes are unequivocally related with the oxidized state of the polymer. In fact, the higher frequency band can be assigned to the C=C stretching vibration of quinoid rings, which is here more intense and shifted to lower wavenumbers than in Fig.3, whereas the 1190 cm<sup>-1</sup> feature is attributed to a combination of quinoid C-N-C stretching and C-H in-plane bending [24,30,31]. The assignment of the 1280 cm<sup>-1</sup> peak is uncertain but, according to previous literature data, it can be attributed to the persistence of persulfate ions which were employed as the oxidizing agent [32]. On the other hand, the occurrence of a reversible oxidation process is supported by the parallel development of the quinone-imine C=N stretching band at 1605 cm<sup>-1</sup>, which appears also slightly downshifted with respect to Fig. 3. Since the quinoid C=C stretching is displaced to lower frequencies, it overlaps with the aromatic C-C stretching of benzenoid rings, that usually appears as an upward band at around 1510 cm<sup>-1</sup> in polyaniline derivatives [21,23]. Therefore, the aromatic C-C stretching band results perturbed and this is probably the reason for the spurious absence of a clear positive feature in the spectra of Fig. 7.

On the other hand, the positive-going band at  $1406\text{ cm}^{-1}$  can be ascribed to an N=N stretching vibration pointing to the formation of azo-derivatives by N-N coupling, as suggested above for the electrochemically synthesized polymer. With regard to the  $1330\text{-}1400\text{ cm}^{-1}$  frequency range, several downward peaks are probably related with different order C-N stretching vibrations of oxidized poly(2A-4TBP). It is worth noting that, in parallel to the electrochemical polymer, quinones are also formed by degradation of this material at  $0.9\text{V}$ , as deduced from the  $1650\text{ cm}^{-1}$  shoulder appearing at such a potential. It can be concluded that, despite some minor differences related with the higher electroactivity of the chemically synthesized polymer, the redox process looks structurally similar for both, chemical and electrochemical materials and, consequently, the species formed upon oxidation are analogous.

To gain more insight on the chemical structure of chemically produced poly(2A-4TBP), an XPS characterization of the sample has been also undertaken. Fig. 8 shows the XPS spectra obtained for C 1s, N 1s and O1s core level signals. In parallel to Fig. 4, the C 1s peak can be fitted with two main contributions at  $284.8$  and  $286.1\text{ eV}$  plus a minor feature at  $288.0\text{ eV}$ . All these peaks appear shifted by  $0.2\text{ eV}$  with respect to Fig. 4 but the assignments match those performed for the electrochemical material. In this way, aromatic carbons are responsible for the  $284.8\text{ eV}$  feature, while that at  $286.1\text{ eV}$  is assigned to carbons bound to either O- or N-containing structures. The main difference between XPS spectra of chemical and electrochemical samples arise from the N 1s signal. The best fit for the chemically synthesized poly(2A-4TBP) is obtained assuming three different contributions with maxima located at  $399.8$ ,  $400.9$  and  $402.1\text{ eV}$ . For the electrochemical film, the higher binding energy peak at  $401.9\text{ eV}$  was attributed to the presence of positively charged N atoms, and such assignment is no different for the chemical material. The feature at  $399.8\text{ eV}$  was related in Fig. 4 with neutral species corresponding to indistinguishable amine, imine and azo groups. In the present spectrum, such a signal can be better resolved giving rise to the intermediate contribution at  $400.9\text{ eV}$ . This latter one is ascribed to nitrogen species having a particular chemical environment, as we will discuss shortly.

On the other hand, the O 1s signal can be deconvoluted into three contributions. The absence of the  $529.8\text{ eV}$  line (see Fig. 4 for a comparison) reveals clearly that the underlying

Pt substrate is in this case not accessible to the radiation, because of the higher thickness of the casted chemical polymer. The high binding energy peak at 533.2 eV reveals the occurrence of C-O-C structures which are part of phenoxazine rings, while the 532.0 eV feature is assigned to those C=O structures materialized at quinoid rings, as it was done for the electrochemical material. The O 1s spectrum presents an additional minor contribution shifted by 2 eV positive to the main O 1s line. That 534.7 eV feature is attributed to the presence of a small amount of water molecules, probably arising from hydrogen bonding to neutral amine/imine sites. This phenomenon seems at the origin of the N 1s signal splitting discussed above, for which the 400.9 eV intermediate peak would result from the partial positive charge at those nitrogen atoms affected by hydrogen bonded water molecules. Similar assignment has been reported recently for poly(*o*-aminophenol) films [26].

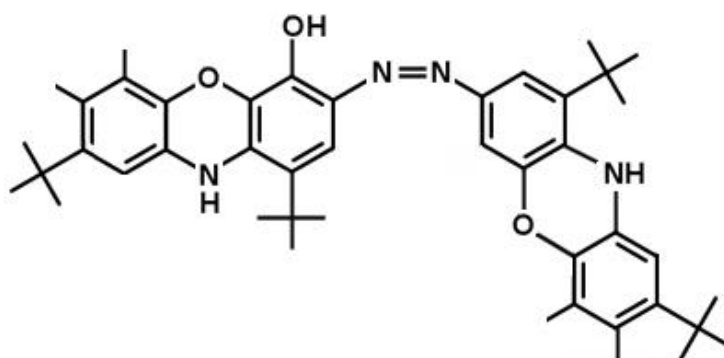
The characterization of the chemically obtained poly(2A-4TB) was complemented by a High-Resolution Mass Spectroscopy study. The HRMS spectrum revealed four intense signals at  $m/z=$  1019, 1619, 2219 and 2820, which were attributed to oligomers containing 6, 9, 13 and 16 monomer units in the presence of some counter-ions.

#### 4. Conclusions

Poly(2-amino-4-tert-butylphenol) has been obtained by means of electrochemical and chemical oxidation methods. The productivity of the electrochemical synthesis is significantly lower because the deposited material forms a low conducting layer on the surface of the platinum electrode that hinders further oxidation of the monomer species. In spite of this, both chemical structure and redox behavior of the polymeric material are not governed by the synthesis method employed, either chemical or electrochemical, as deduced from the analysis of the spectroscopic results obtained.

*In situ* FTIR and *in situ* UV-vis spectroscopies strongly suggest that the chemical structure of poly(2A-4TBP) contains both phenoxazine rings and azo moieties. The former, which are more prevalent, arise from the usual *para*-coupling of aniline-derivative monomers while the latter are probably stimulated by the presence of a voluminous alkyl group adjacent to the more reactive *para*- position.

HRMS results revealed the chemical polymerization product as an oligomer mixture containing a maximum of 16 monomer units. The scheme below represents the reduced form of a shorter fragment containing both azo and phenoxazine chemical structures.



According to the chemical structure proposed, it is expected that the redox switching of poly(2A-4TBP) could be almost parallel to that reported for the parent poly(*o*-aminophenol), with small differences ascribed to the presence of some azo groups along the ladder oligomer structure. Indeed, the *in situ* FTIR results presented here reveal that the redox transition of poly(2A-4TBP) involves nearly the same vibrational modes than those reported

for poly(*o*-aminophenol). In addition to the reversible redox transition, the formation of overoxidized structures containing quinone-like structures has been also detected by FTIR, while UV-vis suggests that these structures are more abundant in the electrochemically obtained material than in the chemical product.

The conductivity of poly(2A-4TBP) is lower than that of poly(*o*-aminophenol) and three orders of magnitude inferior to poly(*o*-toluidine). According to this result, the key factor governing the poor poly(2A-4TBP) conductivity seems the formation of azo groups (which can break the extended conjugation) and, probably, not the eventual torsion angle between adjacent rings that relieves the steric strains promoted by the *tert*-butyl group. UV-vis transient species related with the polymer main oxidation peak seem absent in poly(2A-4TBP), yet they play a significant role in the electrical conductivity of the parent poly(*o*-aminophenol) polymer.

## Acknowledgments

Financial support from the Spanish Ministerio de Economía y Competitividad and FEDER funds (MAT2013-42007-P) and from the Generalitat Valenciana (PROMETEO2013/038) is gratefully acknowledged. M. Abidi thanks the Ministry of Higher Education and Scientific Research of Tunisia for funding her stay at the University of Alicante.

## References

- [1] C. Barbero, J.J. Silber, L. Sereno, Formation of a novel electroactive film by electropolymerization of ortho-aminophenol, *J. Electroanal. Chem. Interfacial Electrochem.* 263 (1989) 333–352.
- [2] B. Habibi, M.H. Pournaghi-Azar, Composite electrodes consisting Pt nano-particles and poly (aminophenols) film on pre-treated aluminum substrate as electrocatalysts for methanol oxidation, *J. Solid State Electrochem.* 14 (2009) 599–613.
- [3] H.J. Salavagione, J. Arias, P. Garcés, E. Morallón, C. Barbero, J.L. Vázquez, Spectroelectrochemical study of the oxidation of aminophenols on platinum electrode in acid medium, *J. Electroanal. Chem.* 565 (2004) 375–383.
- [4] H.A. Menezes, G. Maia, Films formed by the electrooxidation of *p*-aminophenol (*p*-APh) in aqueous medium: What do they look like?, *J. Electroanal. Chem.* 586 (2006)

- 39–48.
- [5] S. Sankarapapavinasam, Permeability and electrocatalytic properties of film prepared by electropolymerization of m-aminophenol, *Synth. Met.* 58 (1993) 173–185.
- [6] K. Chiba, T. Ohsaka, Y. Ohnuki, N. Oyama, Electrochemical preparation of a ladder polymer containing phenazine rings, *J. Electroanal. Chem. Interfacial Electrochem.* 219 (1987) 117–124.
- [7] K. Jackowska, J. Bukowska, A. Kudelski, Electro-oxidation of o-aminophenol studied by cyclic voltammetry and surface enhanced Raman scattering (SERS), *J. Electroanal. Chem.* 350 (1993) 177–187.
- [8] X.-G. Li, M.-R. Huang, W. Duan, Y.-L. Yang, Novel Multifunctional Polymers from Aromatic Diamines by Oxidative Polymerizations, *Chem. Rev.* 102 (2002) 2925–3030.
- [9] Y. Wei, R. Hariharan, S.A. Patel, Chemical and electrochemical copolymerization of aniline with alkyl ring-substituted anilines, *Macromolecules.* 23 (1990) 758–764.
- [10] M. Leclerc, J. Guay, L.H. Dao, Synthesis and characterization of poly(alkylanilines), *Macromolecules.* 22 (1989) 649–653.
- [11] S. Cattarin, L. Doubova, G. Mengoli, G. Zotti, Electrosynthesis and properties of ring-substituted polyanilines, *Electrochim. Acta.* 33 (1988) 1077–1084.
- [12] O.. Dimitriev, Origin of the exciton transition shift in thin films of polyaniline, *Synth. Met.* 125 (2001) 359–363.
- [13] C.H.B. Silva, D.C. Ferreira, R.A. Ando, M.L.A. Temperini, Aniline-1,4-benzoquinone as a model system for the characterization of products from aniline oligomerization in low acidic media, *Chem. Phys. Lett.* 551 (2012) 130–133.
- [14] Y. Xia, J.M. Wiesinger, A.G. MacDiarmid, A.J. Epstein, Camphorsulfonic Acid Fully Doped Polyaniline Emeraldine Salt: Conformations in Different Solvents Studied by an Ultraviolet/Visible/Near-Infrared Spectroscopic Method, *Chem. Mater.* 7 (1995) 443–445.
- [15] R.I. Tucceri, C. Barbero, J.J. Silber, L. Sereno, D. Posadas, Spectroelectrochemical study of poly-o-aminophenol, *Electrochim. Acta.* 42 (1997) 919–927.
- [16] A. Wen, T.C.; Sivakumar, C.; Gopalan, In situ, UV–Vis spectroelectrochemical studies on the initial stages of copolymerization of aniline with diphenylamine-4-sulphonic acid, *Electrochim. Acta.* 46 (2001) 1071–1085. doi:10.1016/S0013-4686(00)00691-5.
- [17] A.-H.A. Shah, R. Holze, In situ UV–vis spectroelectrochemical studies of the copolymerization of o-aminophenol and aniline, *Synth. Met.* 156 (2006) 566–575.
- [18] A.-H.A. Shah, R. Holze, Spectroelectrochemistry of two-layered composites of polyaniline and poly(o-aminophenol), *Electrochim. Acta.* 53 (2008) 4642–4653.
- [19] G. Socrates, *Infrared and Raman characteristic group frequencies: Tables and charts.*, 3rd Ed., John Wiley & Sons, Chichester, UK, 2004.
- [20] M. Trchová, J. Stejskal, Polyaniline: The infrared spectroscopy of conducting polymer nanotubes (IUPAC Technical Report), *Pure Appl. Chem.* 83 (2011) 1803–1817.
- [21] I. Seděnková, J. Stejskal, M. Trchová, In Situ Infrared Spectroscopy of Oligoaniline Intermediates Created under Alkaline Conditions., *J. Phys. Chem. B.* 118 (2014) 14972–14981.



- [22] M.A. Cotarelo, F. Huerta, R. Mallavia, E. Morallón, J.L. Vázquez, On the polymerization of 2-aminodiphenylamine, *Synth. Met.* 156 (2006) 51–57.
- [23] M.A. Cotarelo, F. Huerta, C. Quijada, R. Mallavia, J.L. Vázquez, Synthesis and Characterization of Electroactive Films Deposited from Aniline Dimers, *J. Electrochem. Soc.* 153 (2006) D114.
- [24] I. Losito, E. De Giglio, N. Cioffi, C. Malitesta, Spectroscopic investigation on polymer films obtained by oxidation of o-phenylenediamine on platinum electrodes at different pHs, *J. Mater. Chem.* 11 (2001) 1812–1817.
- [25] M.E. Carbone, R. Ciriello, S. Granafei, A. Guerrieri, A.M. Salvi, Electrosynthesis of conducting poly(o-aminophenol) films on Pt substrates: a combined electrochemical and XPS investigation, *Electrochim. Acta.* 144 (2014) 174–185.
- [26] J.F. Watts, High resolution XPS of organic polymers: The Scienta ESCA 300 database. G. Beamson and D. Briggs. John Wiley & Sons, Chichester, ISBN 0471 935921, (1992), *Surf. Interface Anal.* 20 (1993) 267–267.
- [27] P. Brant, R.D. Feltham, X-ray photoelectron spectra of aryldiazo derivatives of transition metals, *J. Organomet. Chem.* 120 (1976) C53–C57.
- [28] H.S.O. Chan, P.K.H. Ho, S.C. Ng, B.T.G. Tan, K.L. Tan, A New Water-Soluble, Self-Doping Conducting Polyaniline from Poly(o-aminobenzylphosphonic acid) and Its Sodium Salts: Synthesis and Characterization, *J. Am. Chem. Soc.* 117 (1995) 8517–8523.
- [29] NIST X-ray Photoelectron Spectroscopy Database, Version 4.1 (Web Version), 2012., [Http://srdata.nist.gov/xps/](http://srdata.nist.gov/xps/). (n.d.).
- [30] M. Trchová, I. Šeděnková, J. Stejskal, In-situ polymerized polyaniline films 6. FTIR spectroscopic study of aniline polymerisation, *Synth. Met.* 154 (2005) 1–4.
- [31] J. Laska, J. Widlarz, Spectroscopic and structural characterization of low molecular weight fractions of polyaniline, *Polymer (Guildf)*. 46 (2005) 1485–1495.

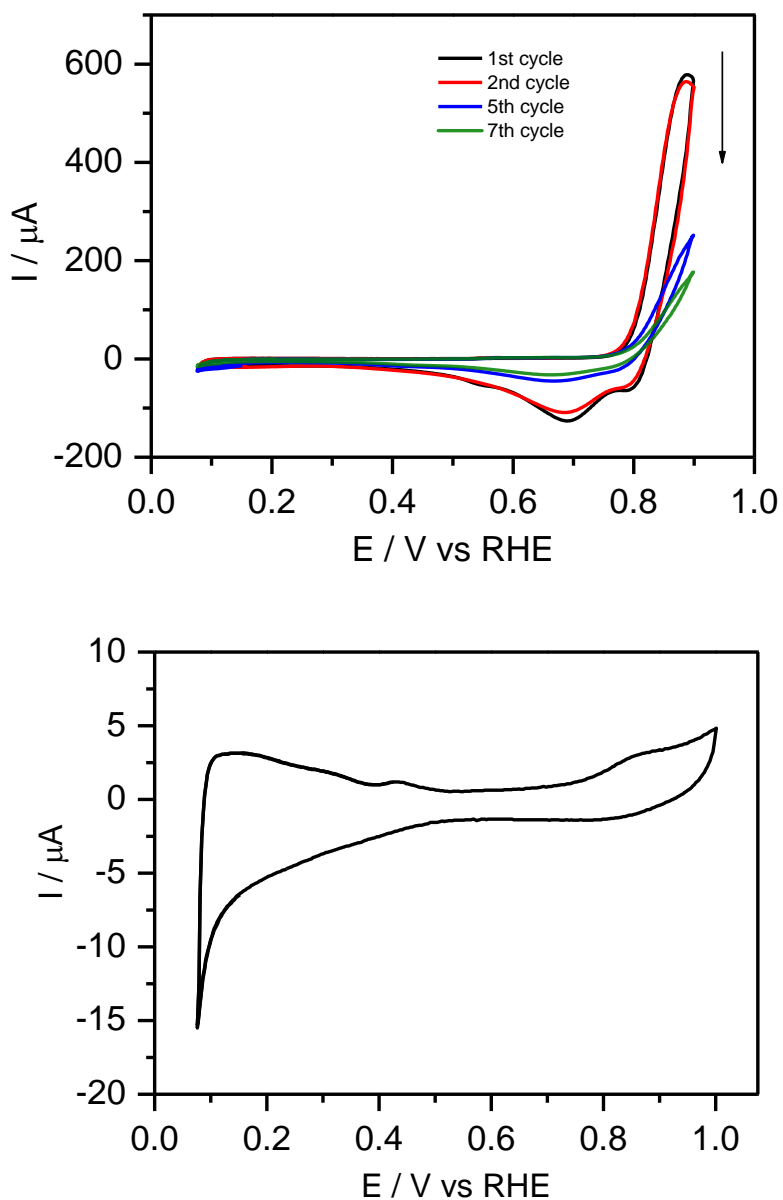


**Fig. 1.** a) Cyclic voltammograms recorded for a Pt electrode during the oxidation of 15 mM 2A-4TBP in 1 M  $\text{HClO}_4$ . b) Electrochemical behavior of a poly(2A-4TBP) thin film formed as in Fig. 1a. Test solution: 0.1M  $\text{HClO}_4$ .  $v= 50 \text{ mV s}^{-1}$

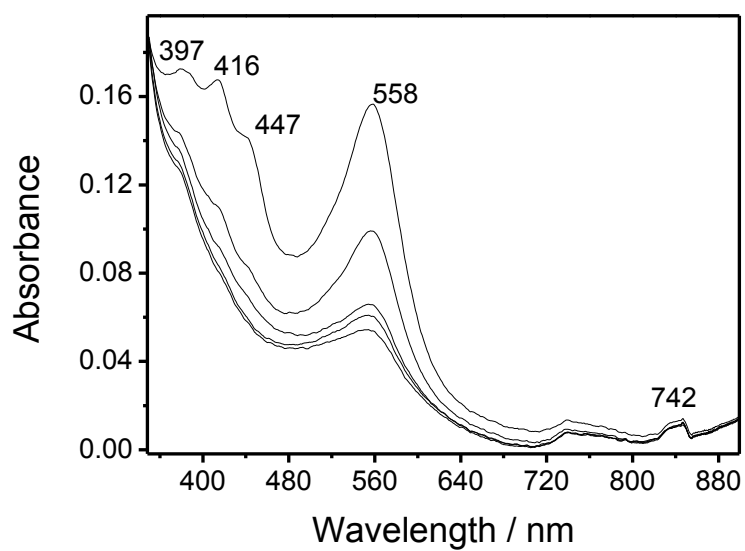


**Fig. 2.** *In situ* UV-vis spectra recorded for a poly (2A-4TBP) film at different applied electrode potentials (from bottom to top: 0.05V, 0.25V, 0.45V, 0.55V, 0.65V). The poly(2A-4TBP) film was prepared on ITO coated glass from a solution containing 15mM monomer in aqueous 0.1 M HClO<sub>4</sub>.

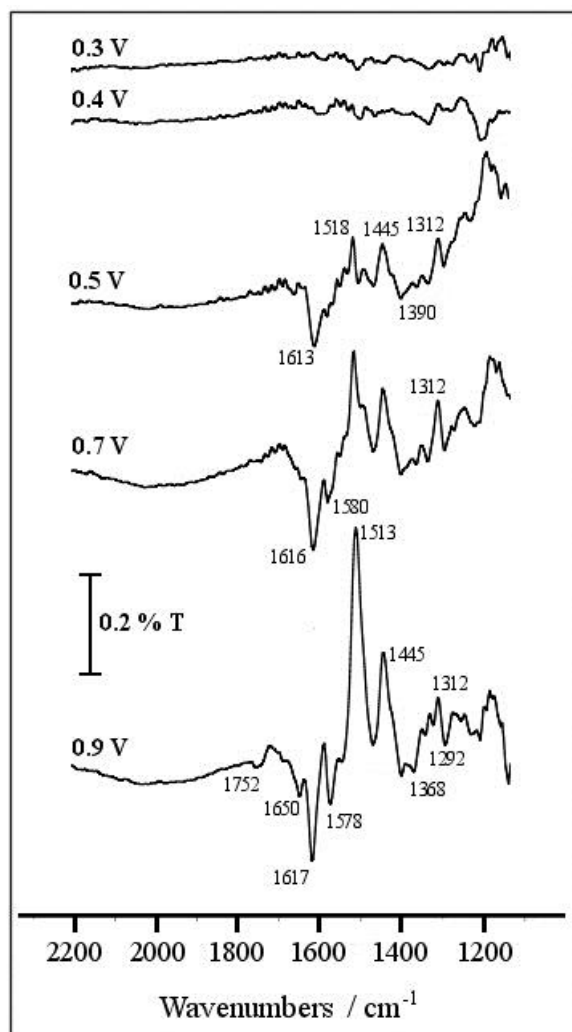


**Fig. 3.** Set of *in situ* FTIR spectra collected during the oxidation of an electrochemically obtained poly(2A-4TBP) film in 0.1M HClO<sub>4</sub>/D<sub>2</sub>O test solution. Reference potential 0.1 V. Sample potential labelled for each spectrum. 100 interferograms at each potential.

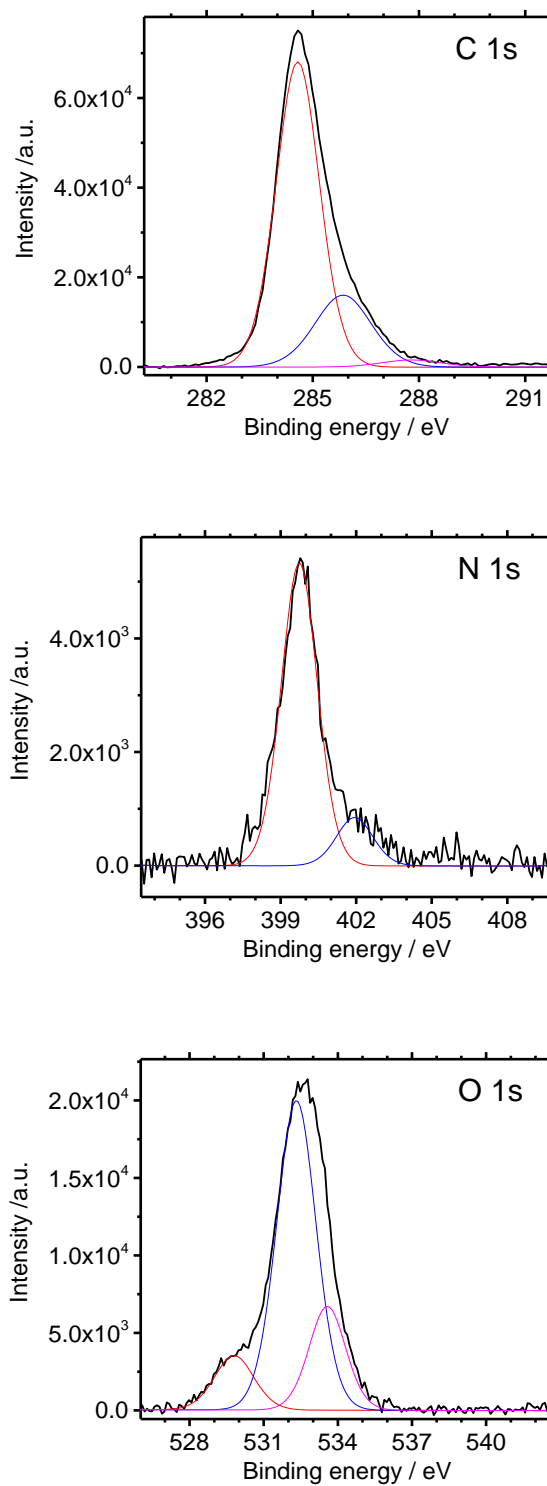


**Fig.4.** High resolution XPS signals for C 1s, N 1s and O 1s obtained from a poly(2A-4TBP) film electrodeposited on a platinum substrate.

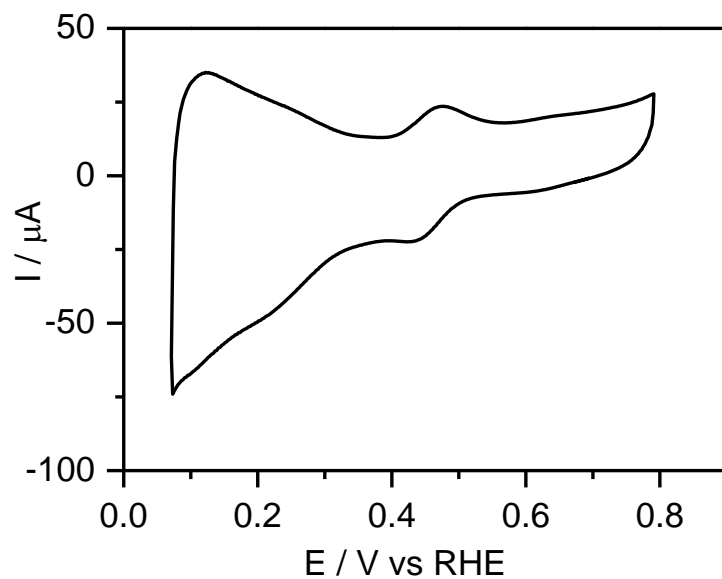


**Fig.5.** Cyclic voltammogram recorded in 0.1M HClO<sub>4</sub> electrolyte for poly(2A-4TBP) synthesized chemically and casted on a polycrystalline platinum electrode.  $v= 50 \text{ mV s}^{-1}$ .

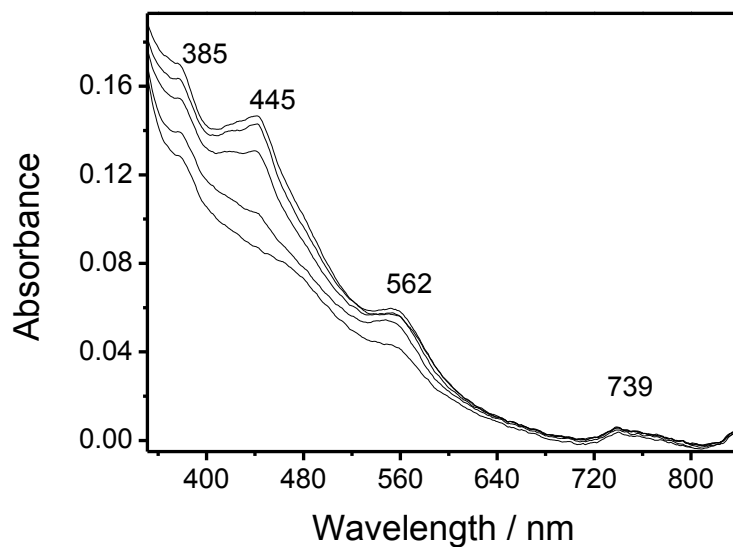


**Fig. 6.** *In situ* UV-vis spectra recorded at different electrode potentials (from bottom to top: 0.05V, 0.25V, 0.45V, 0.55V, 0.65V) for a chemically synthesized poly (2A-4TBP) deposited on ITO. Test solution 0.1M HClO<sub>4</sub>.

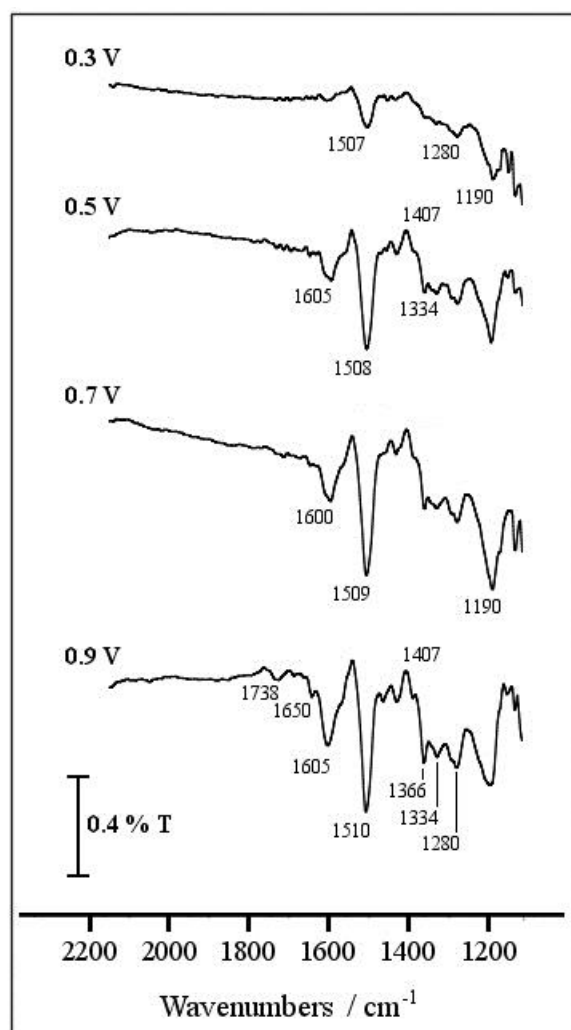


**Fig. 7.** *In situ* FTIR spectra collected during the oxidation of a chemically synthesized poly(2A-4TBP) in 0.1M HClO<sub>4</sub>/D<sub>2</sub>O test solution. Reference potential 0.1 V. Sample potential labelled for each spectrum. 100 interferograms at each potential.

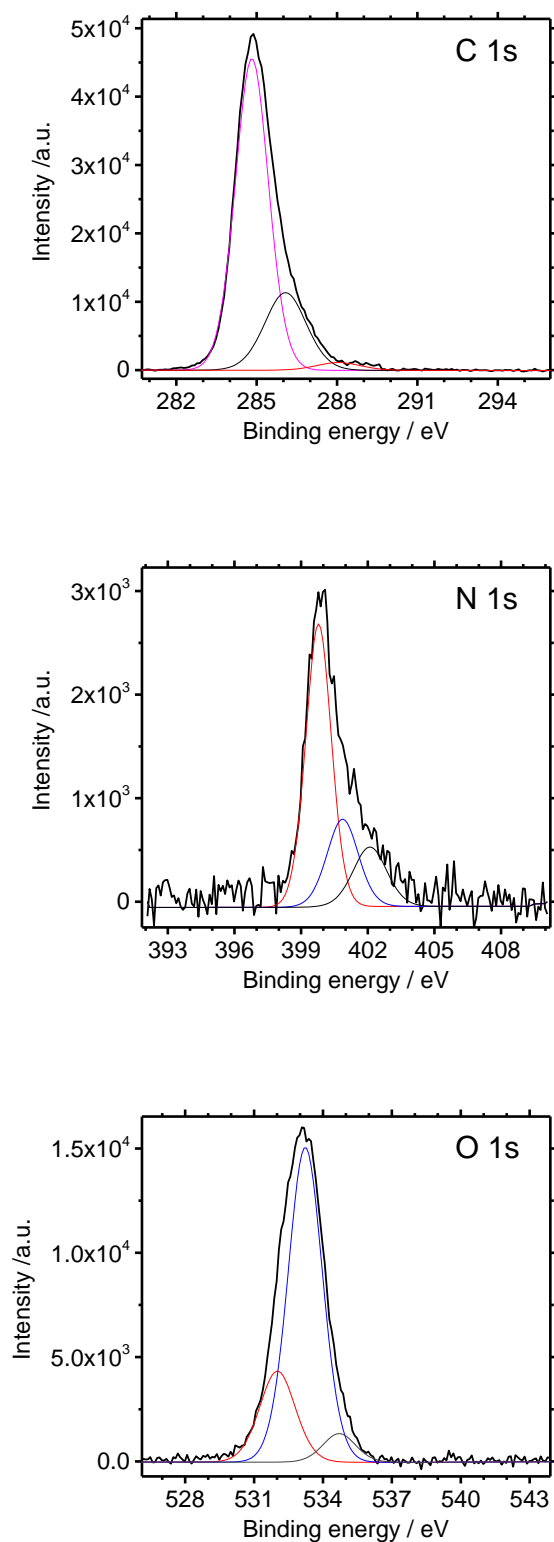
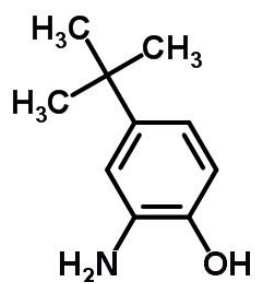


**Fig. 8.** High-resolution XPS spectra of chemically synthesized poly (2A-4TBP) showing the curve-fitted signals for C 1s, N 1s and O 1s.





Scheme 1: Chemical structure of 2-amino-4-tert-butylphenol (2A-4TBP)

**Table 1.** Observed frequencies and proposed assignments for the vibrational bands of electrochemically deposited poly (2A-4TBP)

	Frequency (cm <sup>-1</sup> )	Assignment	Ref.
<b>Reduced state</b>	1518	Aromatic C-C str.	[3][19]
	1445	Azo group N=N str.	[22]
	1312	Secondary aromatic amine N-H str.	[23]
<b>Oxidized state</b>	1752	Carboxylic acid C=O str.	[3]
	1650	Quinone C=O str	[3]
	1617	Quinone-imine C=N str.	[24]
	1578	Quinoid ring C=C str.	[20]
	1330-1400	Intermediate order (C≈N) str.	[23]
	1292	Carboxylic acid C-OH str.	[20]

**Table 2.** Proposed assignments for the main vibrational bands of chemically synthesized poly(2A-4TBP) in 0.1M HClO<sub>4</sub> / D<sub>2</sub>O.

	Frequency (cm <sup>-1</sup> )	Assignment
<b>Reduced state</b>	1407	N=N str.
<b>Oxidized state</b>	1738	Carboxylic acid C=O str.
	1650	Quinone C=O str.
	1605	Quinone-imine C=N str
	1507	Quinoid ring C=C str.
	1330-1400	Intermediate order (C≈N) str.
	1280	S <sub>2</sub> O <sub>8</sub> <sup>2-</sup>
	1190	N-C-N str. + C-H bend.